Available online at www.ijpe-online.com

International Journal of Performability Engineering

vol. 15, no. 1, January 2019, pp. 138-145
DOI: 10.23940/ijpe.19.01.p14.138145

Health Status Comparisons of Lithium-Ion Batteries When Fusing Various Features

Xueling Hao[a], Yongquan Sun[a,b,*], Zimei Su[a], and Bo Liu[a]

[a]*Institute of Sensor and Reliability Engineering (ISRE), Harbin University of Science and Technology, Harbin, 150080, China*
[b]*Center for Advanced Life Cycle Engineering (CALCE), University of Maryland, College Park, 20742, USA*

Abstract

In order to solve the one-sidedness problem based on a single indicator for evaluating the status of health (SOH) and predicting the remaining useful life (RUL) of lithium-ion batteries, a new algorithm is developed where the different features are integrated on the basis of the beta function distribution. The data of the capacity, internal resistance, and constant current charging time (CCCT) of lithium-ion batteries are analyzed, and then the fused features are presented. The simulation includes the data fusion of different types of batteries and the comparison between the SOH of a single indicator and the SOH of two or three fused indicators. From the simulation results, the end-of-life of the three features after fusion is shorter than the capacity, which indicates that multi-indicators are closer to the real situation than a single indicator for SOH and RUL.

Keywords: lithium-ion battery; SOH; the integration of different features; beta distribution function

(Submitted on October 6, 2018; Revised on November 16, 2018; Accepted on December 18, 2018)

1. Introduction

Energy crisis and environmental concerns are urgent problems that need to be solved for the world's sustainable development [1-3]. Lithium-ion batteries are regarded as the most promising energy candidate, owing to their high energy density, long cycle life, and low self-discharge, and they have been widely employed in hybrid electric vehicles (HEVs), smart grids, and aircraft energy storage systems [4]. With the increase in market demand, high safety and reliability have become the basic requirements for lithium-ion batteries [5]. The battery management system (BMS) is a fundamental element to make battery operation safe, reliable, and efficient [6-7]. The two key tasks in BMS are to estimate SOH and predict RUL to avoid battery abuse and prolong its life span [8-10]. Some studies show that the internal resistance can be the SOH indicator [11], and some researchers have advocated for other indicators, such as the diffusion capacitance [12].

Most researchers have estimated SOH or predicted RUL of lithium-ion batteries with a single feature (capacity or internal resistance). Although this method is used extensively, the results are inaccurate because there are many factors that affect SOH or RUL. RVM is employed with the input of CCCT and AT for on-board capacity estimation of lithium-ion batteries [13]. Nick pointed out that constant CCCT and constant voltage charging time (CVCT) impacted the SOH, and four features were fused to obtain an integrated SOH [14-15]. It was found that constant CCCT and the capacity have a strong linear correlation when the capacity is more than 80% of its rated value, during which the battery is considered healthy. Thus, this paper employs CCCT as the SOH indicator. In this paper, a newly integrated SOH indicator is developed with the help of the beta distribution function from the point of view of capacity and power requirements. We compare the results of SOH integration of different features (including fusion of two features and fusion of three features).

SOH is an integration measure reflecting the current status of a battery in comparison with its fresh status [16]. Lithium-ion battery degradation occurs mainly in properties of the battery, and a loss of lithium-ions will lead to the decline in capacity and the rise in impedance [17]. An increase in internal resistance will be accompanied by a decline in energy density, voltage, and power [18]. The fundamental reason for capacity fade is the failure of the material, and it is closely

* Corresponding author.
E-mail address: 1252339448@qq.com

connected with objective factors such as the battery manufacturing process and the use environment [19]. From the material point of view, the reduction of battery capacity is mainly due to the structure of the cathode material, the SEI transition growth of the negative surface, electrolyte decomposition, metamorphism, collector fluid corrosion, and so on [20]. The capability of power output is determined by both the capacity and the internal resistance. In the process of using the lithium-ion battery, the internal resistance has different changes with the state of charge/discharge (SOC), working environment, life assessment, and state of health (SOH) estimates [20]. Synchrotron radiation technology is the potential lag and voltage decay factor [21]. The fundamental material anomalies are the fundamental factors that increase the internal resistance and battery polarization. Therefore, only using a single feature, such as capacity or internal resistance, to estimate the SOH of the battery is incomprehensive [14]. SOH estimation based on CVCT or CCCT is inaccurate without compensation for discharge depth. So far, many researchers have studied SOH estimation using capacity or internal resistance separately. In order to study the problem of the degree of influence of different indicators, in this paper, we used the beta distribution function to fuse multiple features, considered the changes of the SOH of the battery, and then compared the results of SOH integration of different features (including the fusion of two features and fusion of three features).

The rest of this paper is organized as follows: Section 2 introduces battery experiments, including the charge-discharge process and the identification of the integrated SOH indicator. Section 3 conducts the calculation method of SOH for various features and the process of integrating with SOH of distinctive features and result analysis. Finally, some conclusions are given in Section 4.

2. Experiments

2.1. Charge/Discharge Process

Each of the three batteries are divided into two types, including 1.1 Ah lithium-ion batteries of CS2 type and 1.35Ah lithium-ion batteries of CX2 type. $LiCoO_2$ mixed with carbon of CS2 type as a conductive additive was used as the cathode, while layered graphite bound together with polypropylene fluoride was used as the anode. $LiCoO_2$ mixed with carbon CX2 type as a conductive additive was used as the cathode, while layered graphite bound together with polypropylene fluoride was used as the anode. Different charge/discharge profiles were used for cycle life testing, as shown in Table 1.

Table 1. Charge/discharge profiles

Battery	Charge profile	Discharge profile
CS2-33 Constant current rate of 0.5C	Constant current charge at 0.55A from 3.8V to 4.2V, constant voltage charge at 4.2V from 1.1A to 0.05A.	Constant current discharge at 1.1A from 4.2V to 2.7V
CS2-38 Constant current rate of 1.0C	Constant current charge at 0.55A from 3.8V to 4.2V, constant voltage charge at 4.2V from 1.1A to 0.05A.	Constant current discharge at 0.55A from 4.2V to 2.7V
CX2-34 Constant current rate of 1.0C	Constant current charge at 0.675A from 3.6V to 4.2V, constant voltage charge at 4.2V from 1.16A to 0.05A.	Constant current discharge at 1.35A from 4.2V to 2.7V

The charge/discharge profile of battery CS2 is shown in Figure 1 and consists of three phases. The first stage is the constant current charging phase. In Figure 1(a), we can see that the constant charging time of the battery gradually decreased with the increasing charge/discharge cycles, but in Figure 1(b), the trend of voltage growth increases, indicating that the extent of battery aging increases as the charge/discharge cycles increase. The second stage is the constant voltage charging stage. The voltage is maintained near the specific value set in the experiment, so the performance is a straight line in Figure 1(b). This is because the charging capacity of the battery increases continuously and the voltage is relatively high, which makes the charging current decrease continuously. From Figure 1(a), the amplitude change trend of the current decreases relatively slowly as the charge/discharge time increases. Due to the increase in the charge/discharge time, the internal resistance increases and the battery ages. The third stage is the unvarying current discharge stage. As shown in Figure 1(a), as the battery charging/discharging time increases, the battery ages gradually, but the trend of voltage decrease is more intense.

2.2. Measurement Data

Figure 2 shows each feature versus cycle for CS2-33, CS2-38, and CX2-34. From the figure, the trends of capacity and CCCT are almost the same, both of which show exponential decay. However, the change of internal resistance is significantly different. For CS2 type batteries, the internal resistance is inclined to increase as the number of cycles increases. For CX2 type batteries, the internal resistance slowly decays as the number of cycles increases.

However, when the number of cycles is on the brink of 100, the internal resistance of CX2-38 increases sharply and then drops sharply. The main factors achieving the internal resistance of lithium-ion batteries are divided into battery-critical materials and battery usage environment. From Figure 2, the biggest factor should be the battery usage environment, such as temperature and humidity.

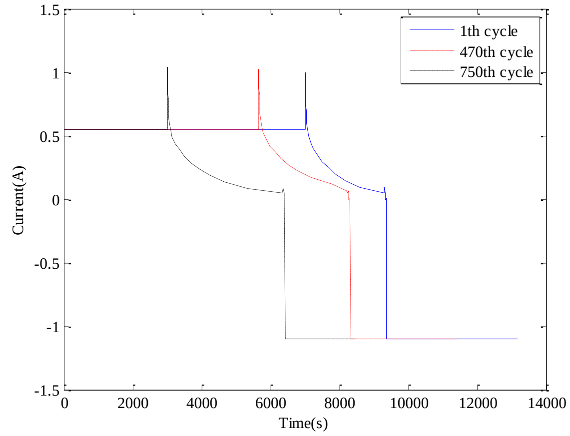

(a)

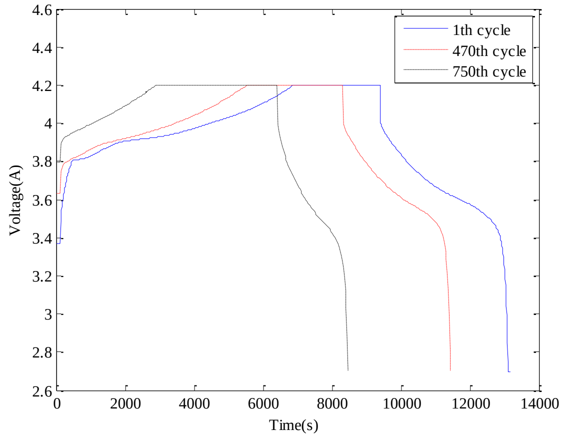

(b)

Figure 1. (a) Current over time features; (b) Voltage over time features

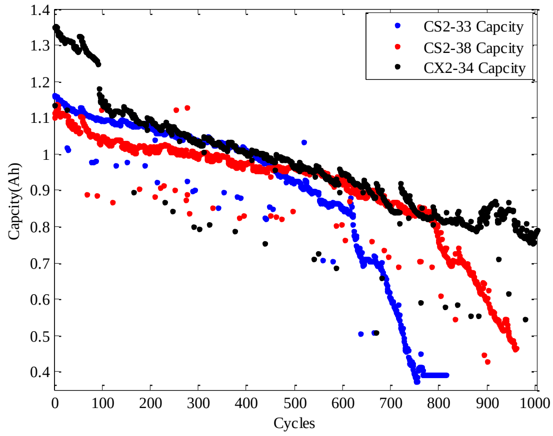

(a) Capacity

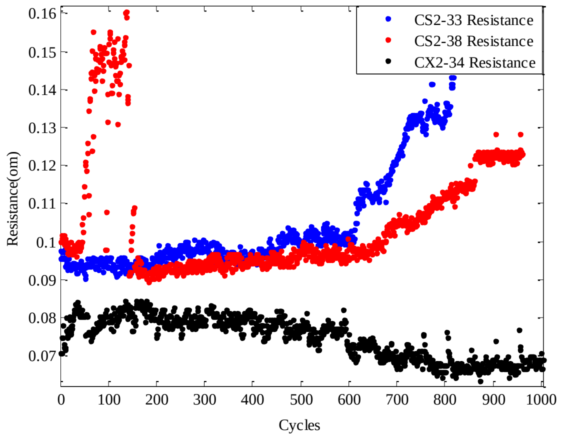

(b) Internal resistance

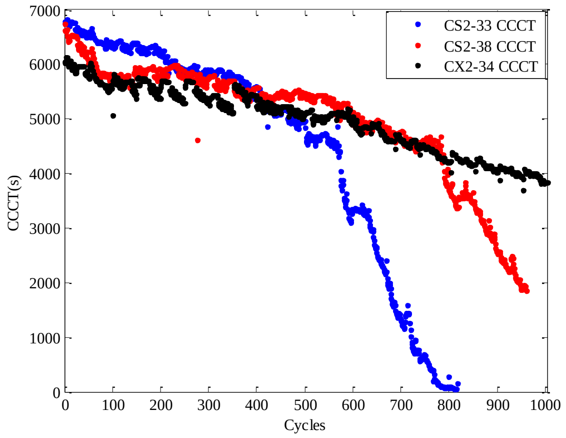

(c) CCCT plotted versus cycles

Figure 2. Each feature

3. The Integration of SOH of Different Features

3.1. SOH Integrated Process

The capacity and CCCT generally increased with the number of cycles, so the formula for CCCT's SOH is consistent with capacity. Currently, capacity is widely used in the field to describe the SOH of lithium-ion batteries, and it can be described as follows:

$$SOH_{cap} = \frac{Capacity(k)}{Capacity(0)} \tag{1}$$

$$SOH_{ccct} = \frac{Time(k)}{Time(0)} \tag{2}$$

Where $Capacity(0)$ denotes the initial capacity of lithium-ion batteries (Ah), $Capacity(k)$ denotes the actual capacity of lithium-ion batteries (Ah), $Time(0)$ denotes the initial time of lithium-ion batteries (s), and $Time(k)$ denotes the actual time of lithium-ion batteries (s). Some researchers proposed the SOH definition based on internal resistance, as follows:

$$SOH_{res} = \frac{R_{eol} - R(k)}{R_{eol} - R_{new}(0)} \tag{3}$$

Where $R_{new}(0)$ denotes the internal resistance of lithium-ion battery (Ω), R_{eol} denotes the internal resistance at the end of life (Ω), and $R(k)$ denotes the internal resistance in the current state (Ω).

In the beta distribution, parameters can be understood as pseudo count and have the same form as the beta; therefore, beta distribution can be used as a prior distribution. The mathematical form of the probability density distribution function of beta distribution is

$$f(x;\alpha,\beta) = \frac{x^{\alpha-1}(1-x)^{\beta-1}}{\int_0^1 \mu^{\alpha-1}(1-\mu)^{\beta-1}\mathrm{d}\mu} = \frac{1}{B(\alpha,\beta)} x^{\alpha-1}(1-x)^{\beta-1} \tag{4}$$

Where $0 < x < 1,\ \alpha > 0,\ \beta > 0$, the variable x can only appear between 0 and 1, and α and β are two parameters greater than 0. $B(\alpha,\beta) = \int_0^1 \mu^{\alpha-1}(1-\mu)^{\beta-1}\mathrm{d}\mu.$

The beta function was employed to incorporate capacity, internal resistance, and CCCT features. The probability density function (PDF) for the battery SOH_{fus} at cycle k is

$$f_k(SOH_{fus\ k};\alpha_k,\beta_k) = \frac{SOH_{fus\ k}^{\alpha_k-1}(1-SOH_{fus\ k})^{\beta_k-1}}{B(\alpha_k,\beta_k)} \tag{5}$$

Where $SOH_{fus\ k}$ is the battery SOH_{fus} at cycle k and α_k and β_k are parameters. The estimates of parameters α_k and β_k are

$$\alpha_k = \sum_{j=1}^{n} w_{j,k} d_{j,k} \tag{6}$$

$$\beta_k = \sum_{j=1}^{n} w_{j,k}(1 - d_{j,k}) \tag{7}$$

Where $d_{j,k}$, (j = 1, 2, ⋯, n) are observations of features at cycle k, n indicates the number of features , j indicates different features, $w_{j,k}$ is the weight of feature $d_{j,k}$, and the initial weights $w_{j,1} = 1/3$ when $k = 1$.

The point estimate of SOH at cycle k is computed by the maximum likelihood of f_k ($SOH_{fus\ k}$; α_k, β_k), as follows:

$$SOH_{fus\ k} = \frac{\alpha_k}{\alpha_k + \beta_k} = \frac{\sum_{j=1}^{n} w_{j,k} d_{j,k}}{\sum_{j=1}^{n} w_{j,k}} \tag{8}$$

When the observations of the features of the next cycle (k + 1) are obtained, the weights are then updated based on the following Equation [11]:

$$w_{j,k+1} = w_{j,k} + (1 - \left| SOH_{fus\ k} - d_{j,k} \right|) \tag{9}$$

3.2. Results and Discussion

Figures 3, 4, and 5 show the features and corresponding SOH. The trend for each feature is different, and the capacity and CCCT show a heavy dependence on the depth of discharge, which would be attributed to increased model complexity and constant recalibration. However, since the linear trend of each feature change is uniform across all batteries, relying solely on a single feature to judge SOH estimation may result in inaccurate estimation of SOH.

3.2.1. The Integration of the Same Battery with Different SOH

In Figures 3 and 4, (a) is the value of SOH_{cap} and SOH_{res} integration, where the integrated SOH_{fus} value is exactly the average of the two, and (b) is the SOH_{cap}, SOH_{res}, and SOH_{ccct} values after integration, and the distribution of the SOH_{fus} values fluctuates between these three eigenvalues. From Figures 3 and 4, the constant current rate of the battery is different. The SOH_{cap} and SOH_{ccct} decay rate or SOH_{res} growth rate is also different. The internal resistance measurements for battery CS2-33 are highly favorable, even more so than in the simplest test conditions shown in battery CS2-38. The internal resistance increases linearly throughout the entire cycle life with less noise than what was found in batteries CS2-38. In addition, for the batteries, which are the same type, the charge/discharge rates and discharge currents will also lead to different SOH and RUL.

According to GB / T31484-2015, in the standard cycle life of “standard cycle life test, the number of cycles up to 500 times the capacity should not be less than 90% of the initial capacity, or the number of cycles up to 1000 times the capacity should not below 80% of the initial capacity”. If the capacity drops sharply within the universal cycle, this is a failure of capacity fade. Since the battery capacity is only currently used to determine the battery failure criteria, and other features do not give the failure criteria, SOH_{fus} and SOH_{cap} can only be reported to analyze the accuracy of the integrated results. From Figure 3(a), if the battery failure time is established according to the above criteria and the number of cycles reaches 294, the SOH_{cap} will start to be lower than 90% of the original SOH_{cap} and the battery is judged as invalid. If the same criterion is used, the SOH_{fus} and SOH_{cap} have some margin of error to determine the failure criteria. When the number of cycles reaches 290, the SOH_{fus} starts to be lower than 90% of the initial SOH_{fus} and the battery is considered failed. Compared with Figure 3(a), Figure 3(b) is the SOH_{fus} integration of the three features SOH_{fus}. When the number of cycles reaches 249, SOH_{fus} will start to be lower than 90% of the initial SOH_{fus}, and the battery is judged as failed. It can be observed that the SOH integration of the three features is better than the SOH integration of the two features.

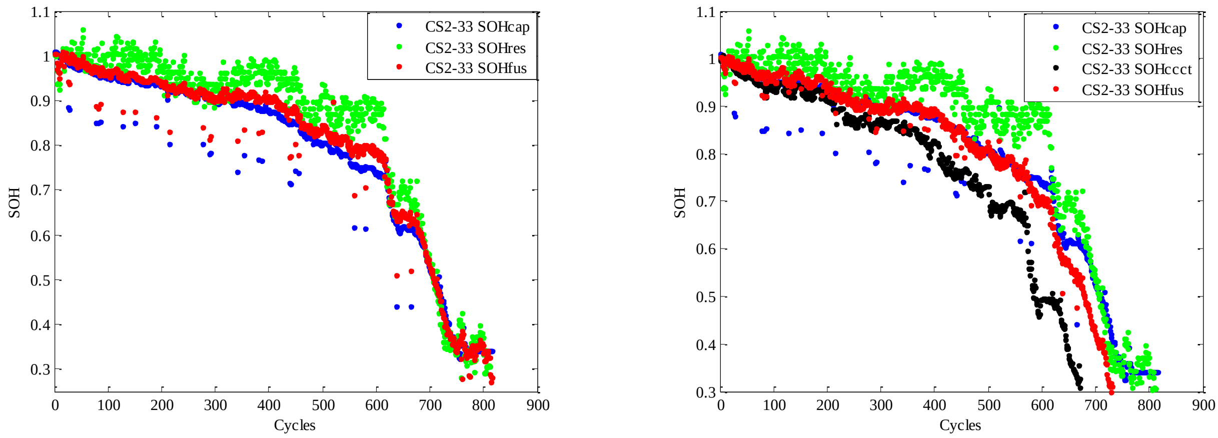

(a) Integrated of SOH_{cap} and SOH_{res} (b) Integrated of SOH_{cap}, SOH_{res}, and SOH_{ccct}

Figure 3. Integration of SOH of different features for battery CS2-33

Due to the different charging/discharging rates, the trend of each feature in Figures 3 and 4 is also different. From Figure 4, if the battery capacity is used to determine the battery failure time, the CS2-38 battery failure time is 125 times the number of cycles. Judging from the integrated point of view, the CS2-38 battery fails when the number of cycles reaches about 100 times. This requires further analysis of the failure mechanism of the battery. In the process of using lithium-ion batteries, because the internal resistance will vary with the state of charge/discharge (SOC) and environment, the cycle times will be different and impact the battery performance testing, life assessments, and state of health (SOH) estimates.

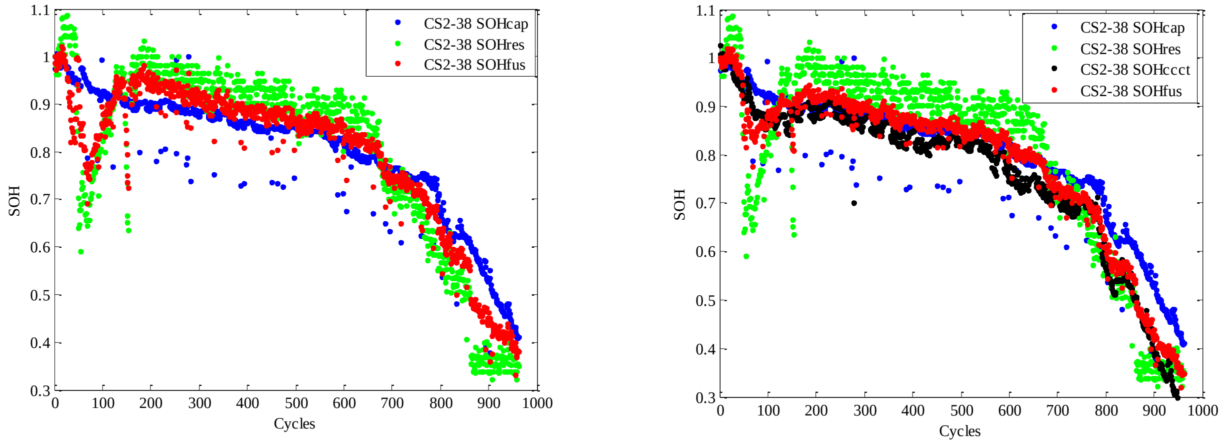

(a) Integration of SOH_{cap} and SOH_{res} (b) Integration of SOH_{cap}, SOH_{res}, and SOH_{ccct}

Figure 4. Integration of SOH of different features for battery CS2-38

3.2.2. The Integration of Different Batteries with Different SOH

Figures 3 and 5 are two different types of battery features of different values of SOH trend. The biggest difference is the trend of internal resistance: for CS2 type batteries, the charging internal resistance increases, while for CX2 type batteries, the charging internal resistance gradually decreases. The fluctuation of the decrease or increase tendency is not large, resulting in the change law. The reason for this is not yet known and requires further study. However, with the trend of this internal resistance change, the traditional ones where the internal resistance increases gradually with the increase in the number of charges/discharges are one-sided. In addition, the CCCT changes of the two types of batteries are also different. For CS2 type batteries, if the CCCT failure threshold is the same as the capacity failure threshold, noted as 90%, the CCCT first reaches the failure threshold as shown in Figure 5(b). For CX2 type batteries, the result is the opposite and the capacity first reach the failure threshold.

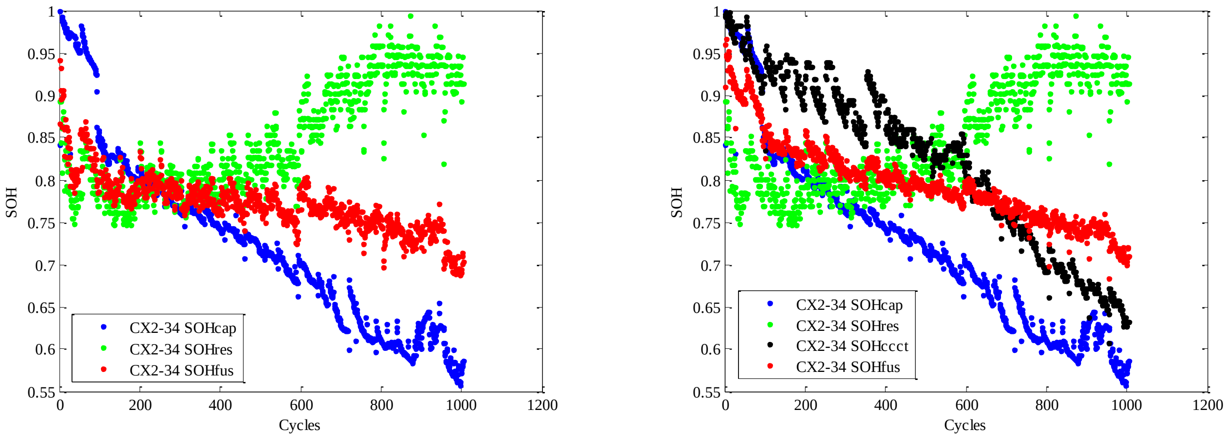

(a) Integration of SOH_{cap} and SOH_{res} (b) Integration of SOH_{cap}, SOH_{res}, and SOH_{ccct}

Figure 5. Integration of SOH of different features for battery CS2-34

4. Conclusions

Observations of the capacity, resistance, and CCCT were extracted from battery cycling experiments, and the variations of these three features were correlated to aging mechanisms. We conclude that the capacity, resistance, and CCCT should be integrated to produce a new SOH indicator from the point of view of capacitance and power. Consequently, a method to integrate this new SOH indicator is developed using the beta function.

In this paper, SOH with different characteristics is fused with the beta function, and fused SOH (including a single feature SOH, two features SOH, and three features SOH) are compared to obtain a comprehensive SOH that will be greatly improved for battery reliability evaluation and BMS systems. This approach also avoids the one-sidedness caused by SOH evaluation of a single feature.

In addition, many researchers often use the internal resistance to evaluate the battery SOH, but for some batteries, the external factors or internal factors have a greater impact on the battery and battery SOH evaluation or RUL of the prediction will be affected, so the use of internal resistance to evaluate the battery SOH or predict the battery RUL has some difficulties.

In this article, only SOH is analyzed and compared. Future works could focus on building a better model for SOH estimation that considers the capacity, internal resistance, and CCCT combined with other identification algorithms. Furthermore, the works could aim to perfectly obtain the capacity, internal resistance, and CCCT characteristics using experimental data at different temperatures.

Acknowledgements

This research was sponsored by the Natural Science Foundation of Heilongjiang Province (No. QC2016068), University Nursing Program for Young Scholars with Creative Talents in Heilongjiang Province (No. UNPYSCT-2017087), and Heilongjiang Provincial Department of Education Research Project (No. HPDERP-12531097). The authors thank CALCE for providing the testing data of batteries.

References

1. K. Chatzizacharia, V. Benekis, and D. Hatziavramidis, “A Blueprint for an Energy Policy in Greece with Considerations of Climate Change,” *Applied Energy*, Vol. 162, pp. 382-389, 2016
2. T. Fujimi, Y. Kajitani, and S. E. Chang, “Effective and Persistent Changes in Household Energy-Saving Behaviors: Evidence from Post-Tsunami Japan,” *Applied Energy*, Vol. 167, pp. 93-106, 2016
3. I. M. Kong, J. W. Choi, S. I. Kim, E. S. Lee, and M. S. Kim, “Experimental Study on the Self Humidification Effect in Proton Exchange Membrane Fuel Cells Containing Double Gas Diffusion Backing Layer,” *Applied Energy*, Vol. 145, pp. 345-353, 2015
4. T. R. Ashwin, Y. M. Chung, and J. H. Wang, “Capacity Fade Modelling of Lithium-Ion Battery under Cyclic Loading Conditions,” *Journal of Power Sources*, Vol. 328, pp. 586-598, 2016
5. J. B. Goodenough and Y. Kim, “Challenges for Rechargeable Li Batteries,” *Chemistry of Materials*, Vol. 22, No. 3, pp. 587-603, 2010
6. L. Lu, X. Han, J. Li, J. Hua, and M. Ouyang, “A Review on the Key Issues for Lithium-Ion Battery Management in Electric Vehicles,” *Power Sources*, Vol. 226, pp. 272-288, 2013
7. X. Zhang, Y. J. Wang, and C. Liu, “A Novel Approach of Remaining Discharge Energy Prediction for Large Format Lithium-Ion Battery Pack,” *Journal of Power Sources*, Vol. 343, pp. 216-225, 2017
8. M. Berecibar, I. Gandiaga, I. Villarreal, N. Omar, J. Van Mierlo, and P. Van den Bossche, “Critical Review of State of Health Estimation Methods of Li-Ion Batteries for Real Applications,” *Renewable and Sustainable Energy Review*, Vol. 56, pp. 572-587, 2016
9. E. Sarasketa-Zabala, E. Martinez-Laserna, M. Berecibar, I. Gandiaga, L. R. Martinez, and I. Villarreal, “Realistic Lifetime Prediction Approach for Li-Ion Batteries,” *Applied Energy*, Vol. 162, pp. 839-852, 2016
10. J. Wu, C. Zhang, and Z. Chen, “An Online Method for Lithium-Ion Battery Remaining Useful Life Estimation using Importance Sampling and Neural Networks,” *Applied Energy*, Vol. 173, pp. 134-140, 2016
11. T. Fen, L. Yang, X. Zhao, H. Zhang, and J. Qiang, “Online Identification of Lithium-Ion Battery Parameters based on an Improved Equivalent Circuit Model and its Implementation on Battery State-of-Power Prediction,” *Power Sources*, pp. 192-203, 2015
12. A. Eddahech, O. Briat, and J. Vinassa, “Determination of Lithium-Ion Battery State-of-Health based on Constant-Voltage Charge Phase,” *Power Sources*, Vol. 258, pp. 218-227, 2014
13. Y. Zhang and B. Guo, “Online Capacity Estimation of Lithium-Ion Batteries based on Novel Feature Extraction and Adaptive Multi-Kernel Relevance Vector Machine,” *Energies*, Vol. 8, No. 11, pp. 12439-12457, November 2015
14. N. Williard, W. He, M. Osterman, and M. Pecht, “Comparative Analysis of Features for Determining State of Health in Lithium-Ion Batteries,” *International Journal of Prognostics and Health Management*, pp. 2153-2648, 2013
15. Y. P. Zhou and M. H. Huang, “On-Board Capacity Estimation of Lithium-Ion Batteries based on Charge Phase,” Journal of *Electrical Engineering and Technology*, Vol. 13, pp. 1921-718, 2018
16. A. E. Mejdoubi, A. Oukaour, and H. Chaoui, “State-of-Charge and State-of-Health Lithium-ion Batteries Diagnosis According to Surface Temperature Variation,” *IEEE Transactions on Software Engineering*, Vol. 63, No. 4, April 2016
17. M. B. Pinson, and M. Z. Bazant, “Theory of SEI Formation in Rechargeable Batteries: Capacity Fade, Accelerated Aging and Lifetime Prediction,” *Electrochem*, Vol. 160, pp. A243-A250, 2012
18. A. Barre, B. Deguilhem, S. Grolleau, M. Gerard, and D. J. Riu, “Failure Analysis of Lithium-Ion Batteries,” *Power Sources*, Vol. 241, pp. 680-689, 2013

19. Q. Y. Wang, S. Wang, and J. N. Zhang, "Overview of the Failure Analysis of Lithium-Ion Batteries," *Energy Storage Science and Technology*, No. 43, pp. 2095-4239, 2017
20. W. S. Li and S. Z. Qiu, "Causes for Capacity Decrease of Li-Ion Batteries," *Chinese Battery Industry*, Vol. 6, No. 1, pp. 21-24. 2001
21. Y. Xing, N. Williard, and K. L. Tsui, "A Comparative Review of Prognostics based Reliability Methods for Lithium Batteries," in *Proceedings of Prognostics and System Health Management Conference*, pp. 1-6, IEEE, 2011

Xueling Hao is currently studying for a Master's degree in electronics and communications engineering at Harbin University of Science and Technology. Her main research interests are reliability engineering and sensor technology.

Yongquan Sun is an associate professor in the School of Measurement Technology and Communication Engineering at Harbin University of Science and Technology. His current research interests include complex system reliability and maintainability, failure mechanisms for electronic devices, and PHM.

Zimei Su is a professor at Harbin University of Science and Technology. His main research interests are reliability engineering and sensor technology.